

PACS numbers: 42.55.Rz; 42.70.Hj; 78.20.Hp
DOI: 10.1070/QE2010v040n01ABEH014205

Influence of the photoelastic effect on the thermal lens in a YLF crystal*

V.V. Zelenogorskii, E.A. Khazanov

***Abstract*. The thermal lens in an YLF crystal is calculated taking into account the anisotropy of the thermal conductivity, elasticity, linear expansion, and refractive index. It is proved that the experimentally observed strong astigmatism of the thermal lens in YLF can be explained only taking into account the photoelastic effect. It is shown that, in an YLF crystal cut so that the optical axis lies in the plane of the rod face, the contribution to the thermal lens is made only by three photoelastic coefficients for the ordinary wave and only by two coefficients for the extraordinary wave. Using these five photoelastic coefficients as fitting parameters, all the known experimental data are quantitatively interpreted.**

Keywords: *photoelasticity, thermal lens, YLF crystal.*

1. Introduction

The average power of solid-state lasers with nearly diffraction-limited divergence is limited mainly by such thermal effects in the active elements as thermal lens and depolarisation. The thermal lens is formed due to three effects: the temperature dependence of the refractive index, the thermal expansion, and the photoelastic effect, the latter usually making insignificant contribution in isotropic crystals. In contrast, depolarisation is caused only by the photoelastic effect. An important advantage of anisotropic crystals compared to isotropic crystals is that the depolarisation of radiation in them is almost absent [1, 2]. This occurs because the natural birefringence is much stronger than the birefringence induced by the photoelastic effect and, hence, the intrinsic polarisations of the crystal are determined only by the orientation of optical axes and do not depend on the transverse coordinates. Recall that the intrinsic polarisation is the polarisation which does not change as the beam propagates through the medium.

One of the most frequently used anisotropic crystals is the YLF crystal. It can be doped with various ions: Nd, Yb, Ho, Tm, Er, Ce, Pr, etc. The most widely used is the Nd : YLF crystal, which has several advantages compared to Nd : YAG, namely, a longer excited-state lifetime (480 μs), a higher saturation energy (1.18 J cm^{-2} [3] for the ordinary and 0.77 J cm^{-2} for the extraordinary wave), a wider gain band, a weaker thermal lens, and a lasing wavelength of 1053 nm (for the ordinary wave), which coincides with the wavelength of neodymium phosphate glass.

YLF is a uniaxial crystal, which shows no thermally induced depolarisation when cut perpendicular to the optical axis (the so-called π-orientation, or *a*-cut, Fig. 1) and, hence, the thermal lens is the only thermal effect in this crystal. The thermal lens in Nd : YLF rods with π-orientation was experimentally studied in several works using both the side [3 – 8] and end [9 – 12] pumping; the measurements in [3 – 8, 10] were performed for both the ordinary (σ polarisation, gain at a wavelength of 1053 nm) and extraordinary (π polarisation, gain at 1047 nm) wavelengths. In [3 – 7], a strong astigmatism of the thermal lens was observed for both wavelengths, i.e., the thermal lens for each polarisation is characterised by two focal lengths: $F_{||}$ for rays propagating in a plane passing through the optical axis and $F_{\perp}$ for rays lying in the perpendicular plane. Thus, the observed thermal lens is completely determined by four focal lengths: $F_{o||}$, $F_{o\perp}$, $F_{e||}$ and $F_{e\perp}$. Hereinafter, the subscripts 'o' and 'e' correspond to the ordinary and extraordinary polarisations of radiation. The experimental data published in papers [3 – 7] are considerably different. In particular, the ratio $F_{e||}/F_{e\perp}$ for the extraordinary wave varies from 1.5 [3] to 7 and higher values [7]. The spread for

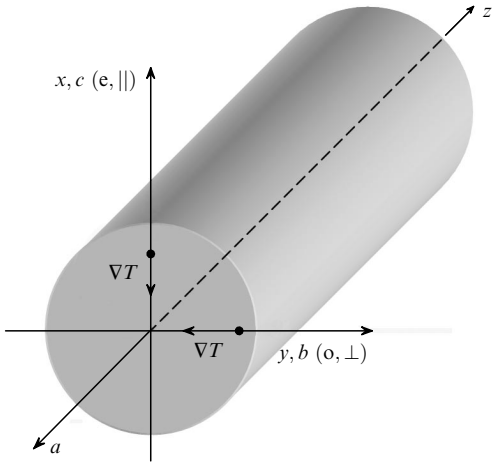

Figure 1. Geometry of a π-oriented (*a*-cut) crystal.

*Reported at the Conference 'Laser Optics 2009', St. Petersburg, Russia.

V.V. Zelenogorskii, E.A. Khazanov Institute of Applied Physics, Russian Academy of Sciences, ul. Ul'yanova 46, 603950 Nizhnii Novgorod, Russia; e-mail: vvmailv@mail.ru

Received 10 August 2009
Kvantovaya Elektronika **40** (1) 40 – 44 (2010)
Translated by M.N. Basieva

the ordinary wave is even greater: the lens in [3] is negative with $F_{o||}/F_{o\perp} = 0.5$, the focal lengths of the lens in [4–6] have different signs ($F_{o||} < 0$, $F_{o\perp} > 0$), and the lens in [7] is cylindrical and positive. The authors of [8–12] do not mention about astigmatism and, obviously, give the mean value of the focal length.

Despite such a large body of experimental data, the authors of [3–7] even qualitatively do not explain the thermal lens astigmatism in Nd:YLF crystals. In [3, 5, 6], the astigmatism nature is not discussed at all. The authors of [4] refer to the anisotropy of the thermal conductivity ($\kappa_{||} < \kappa_{\perp}$, where κ is the thermal conductivity coefficient)*, but this anisotropy would lead to $|F_{e||}| < |F_{e\perp}|$, while all experiments show $|F_{e||}| > |F_{e\perp}|$. The contribution of thermal expansion to the thermal lens in long rods is insignificant, and, in addition, the astigmatism of this component is small. The authors of [7] explain the astigmatism by the fact that, in their experiments, the size of the pump beam cross section along the optical axis c was 1.5-fold larger than in the perpendicular direction. However, this can lead to the focal length ratio of 2.25, which is considerably smaller than the values given in the work. Finally, the explanation of the thermal lens astigmatism by the refractive index anisotropy ($n_o \neq n_e$, $dn_o/dT \neq dn_e/dT$) is completely groundless because the astigmatism is a phenomenon that occurs for radiation of one polarisation and is observed for the o- and e-waves independently of each other.

We believe that the only cause of the thermal lens astigmatism is the photoelastic effect, which was not even mentioned in works [3–9, 11–12] and was mistakenly neglected in [10] based on the absence of depolarisation in anisotropic crystals. The reasonable neglect of the contribution of the photoelastic effect to depolarisation [1, 2] in no way allows one to disregard its contribution to the thermal lens. In other words, the photoelastic effect does not change the intrinsic polarisations of crystals with natural anisotropy, but can substantially change the refractive indices for radiation with these polarisations. These changes are principally astigmatic because the angle between the optical axis and the temperature gradient (the source of the photoelastic effect) is different at different points of the crystal cross section.

In this work, we precisely calculate the thermal lens in an YLF crystal taking into account the anisotropy of the thermal conductivity, elasticity, linear expansion, and refractive index. It is proved that, neglecting the photoelastic effect, it is impossible to explain numerous experimental data even qualitatively. It is shown that the contribution to the thermal lens is made by only three photoelastic coefficients for the ordinary wave and by only two coefficients for the extraordinary wave. Using these five photoelastic coefficients as fitting parameters (their values are not given in the literature), we have quantitatively interpret all experimental data.

2. Formulation of the problem

The thermal lens in an optical element is formed by a volume heat source, which, in our case, is the pump radiation absorbed in the crystal. The need to remove heat through the sample surface leads to the appearance of a temperature gradient. The inhomogeneous temperature field $T(x, y, z)$ forms a displacement field $\boldsymbol{U}(x, y, z)$ in the crystal. The temperature and deformations determine variations in the refractive index and the sample shape, which, in turn, specify the phase incursion for radiation passing through the sample. This is the phase incursion inhomogeneity over the sample aperture that is responsible for the appearance of the thermal lens under study.

In this paper, we restrict ourselves to the consideration of a steady-state case. The steady-state temperature distribution is determined by the balance equation for heat fluxes in the sample,

$$\operatorname{div}(K \operatorname{grad} T) + Q = 0, \tag{1}$$

where Q is the volume density of heat sources and T is the temperature. In contrast to isotropic materials, the thermal conductivity is determined by the second-rank tensor K rather than by a figure. The sample is not exposed to external volume forces and, hence, the internal stress forces under equilibrium conditions must be mutually compensated in each element of the sample volume. Thus, the balance equation of a deformed sample has the form

$$\frac{\partial \sigma_{ij}}{\partial q_j} = 0, \quad i,j = 1, 2, 3, \tag{2}$$

where σ_{ij} is the stress tensor and q_j are the coordinates of any Cartesian system. Hereinafter, we mean the summation over recurring indices. The stress tensor σ_{ij} for an inhomogeneous temperature distribution can be expressed via the linear thermal expansion tensor α_{ij}, the elasticity tensor C_{ijkl} (fourth-rank tensor), and the deformation tensor u_{ij}, which is determined by the displacement field $\boldsymbol{U}$:

$$\sigma_{ij} = C_{ijkl}(u_{kl} - \alpha_{kl} T), \tag{3}$$

$$u_{ij} = \frac{1}{2}\left(\frac{\partial U_i}{\partial q_j} + \frac{\partial U_j}{\partial q_i}\right). \tag{4}$$

In the absence of external surface forces applied to the sample, we can write the zero boundary conditions

$$\sigma_{ij} s_j = 0, \tag{5}$$

where $\boldsymbol{s}$ is the normal to the sample surface. From Eqns (2)–(4), we can derive a system of three equations for U_i. Solving this system with allowance for the boundary conditions (5), we find the displacement field, substitute it into (4), and obtain the deformation tensor u_{ij}.

Knowing u_{ij} and T, we find the relative permittivity tensor ε_{ij} taking into account the small perturbations associated with the refractive index temperature dependence and the photoelasticity effect [1]:

$$\varepsilon_{ij} = \varepsilon_{0ij} + 2\delta_{ij} n_i \frac{dn_i}{dT} T - \varepsilon_{0ik} B_{kl} \varepsilon_{0lj}, \tag{6}$$

where

$$B_{kl} = p_{klij} u_{ij}; \tag{7}$$

*Hereinafter, the values with the subscripts || and ⊥ characterise the properties of the medium along (||) and perpendicular (⊥) to the optical axis c.

ε_{0ij} is the unperturbed relative permittivity tensor; $n_i = \sqrt{\varepsilon_{0ij}}$ is the unperturbed refractive index for the wave polarised along the corresponding crystallographic axis; p_{klij} is the photoelasticity tensor (fourth-rank tensor); and δ_{ij} is the Kronecker delta; summation over i in (6) is not performed. Note also that formulae (2)–(5) are valid in any Cartesian coordinate system and do not change their form with rotation of the system. At the same time, expressions (6), (7) can be applied only to the coordinate system whose axes coincide with the crystallographic axes a, b, c. The ε_{0ij} tensor in this coordinate system has a diagonal form. To calculate the ε_{ij} tensor in the laboratory coordinate system xyz, we must first find it by formula (6) and then use the matrix transformation formulae for rotation of the coordinate system [13, 14]. The relative position of the laboratory (xyz) and crystallographic (abc) coordinate systems is shown in Fig. 1.

In the general case, solving the problem of eigenvectors of the ε_{0ij} tensor, one can find the intrinsic polarisations and refractive indices at each point of the medium and then solve the problem of radiation propagation. For naturally anisotropic crystals, this approach is applicable only to the samples cut along the optical axis (the c-cut) or at a small angle to it. Such YLF crystals were used in, for example, [3, 15–17]. In this work, we consider only the crystals cut so that the optical axis c lies in the plane of the rod face (Fig. 1). For these crystals, the influence of the photoelastic effect on the intrinsic polarisations can be neglected [1, 2], i.e., the effect of nondiagonal elements of the third term in (6) on the ε_{0ij} tensor eigenvectors is weak. It is also easy to show that the effect of these nondiagonal elements on the refractive index of eigenwaves can also be neglected , i.e., the ε_{ij} tensor can be considered to be diagonal, as well as the ε_{0ij} tensor. Then, using (6), we can find the phase of radiation passed through the crystal with a length l as

$$\varphi_p(x,y) = k\int_0^l \frac{\mathrm{d}n_r}{\mathrm{d}T}T\,\mathrm{d}z - \frac{kn_r^3}{2}\int_0^l B_{rr}\mathrm{d}z + k(n_r-1)$$

$$\times\int_0^l u_{33}\mathrm{d}z, \quad p = \mathrm{o},\mathrm{e}; \quad r = 1,2. \tag{8}$$

Here, $r = 1$ for the ordinary wave and $r = 2$ for the extraordinary wave; $k = 2\pi/\lambda$; λ is the wavelength; and tensors B and u in this expression were taken in the laboratory coordinate system xyz. Thus, an additive contribution to the thermally-induced phase is made by three effects: the temperature dependence of the refractive index, the dependence of the refractive index on deformations (photoelastic effect), and the temperature-induced increase in the length. These effects are described by the corresponding three terms in formula (8).

To numerically calculate the temperature T and the deformation tensor u_{ij}, we used the method of finite elements. The program was tested for particular cases with the known analytical solutions, namely, for cubic crystals in the disc and rod geometries. The discrepancy in all the tested cases did not exceed ±0.5 %. The found values of T and u_{ij} were substituted into expression (8). For a uniform heat source [$Q(x,y) = \mathrm{const}$] in a long rod, the dependence of the thermally induced phase φ_p on the x and y coordinates is close to parabolic. This is not the general case, but, when quantitatively describing the thermal lens, we will characterise it by two focal lengths corresponding to the parabolic distribution that most exactly describes the distribution of the phase φ_p in the centre of the crystal. Thus, the thermal lens is characterised by four focal lengths, $F_{\mathrm{o}\|}$, $F_{\mathrm{o}\perp}$, $F_{\mathrm{e}\|}$ and $F_{\mathrm{e}\perp}$.

3. Results of calculations without taking into account the photoelastic effect

It is convenient to describe the focal power of the thermal lens in an anisotropic long rod analogously to the lens power in an isotropic long rod [1]:

$$\frac{1}{F_{o,e;\|,\perp}} = \frac{P_{\mathrm{heat}}}{2S\kappa_{\|,\perp}}P_{\mathrm{o,e};\|,\perp}. \tag{9}$$

Here, $P_{\mathrm{heat}} = \int_V Q\mathrm{d}V$ is the heat release power in the entire sample volume V; S is the square of the crystal aperture; and $P_{\mathrm{o,e};\|,\perp}$ is the thermooptical constant, which, according to (8), is additively contributed by three effects: the temperature dependence of the refractive index ($N_{\mathrm{o,e};\|,\perp}$), the photoelastic effect ($E_{\mathrm{o,e};\|,\perp}$), and the increase in the length with heating ($L_{\mathrm{o,e};\|,\perp}$),

$$P_{\mathrm{o,e};\|,\perp} = N_{\mathrm{o,e};\|,\perp} + E_{\mathrm{o,e};\|,\perp} + L_{\mathrm{o,e};\|,\perp}. \tag{10}$$

In calculations, we used the known parameters of the YLF crystal [18, 19] listed below.

Refractive indices [19]:
- n_{o} 1.448
- n_{e} 1.470

Temperature coefficients of the refractive index (at a constant density)/K^{-1} [19]:
- $\mathrm{d}n_{\mathrm{o}}/\mathrm{d}T$ . . . . . -2.0×10^{-6}
- $\mathrm{d}n_{\mathrm{e}}/\mathrm{d}T$ . . . . . -4.3×10^{-6}

Linear thermal expansion coefficients/K^{-1} [18]:
- $\alpha_{\|}$ . . . . . 13×10^{-6}
- $\alpha_{\perp}$ . . . . . 8×10^{-6}

Thermal conductivity coefficients/W $\mathrm{K}^{-1}\mathrm{m}^{-1}$ [19]:
- $\kappa_{\|}$ 5.8
- $\kappa_{\perp}$ 7.2

Components of the elasticity tensor/GPa [19]:
- C_{11} 121
- C_{12} 60.9
- C_{13} 52.6
- C_{16} . . . . . −7.7
- C_{33} 156
- C_{44} 40.9
- C_{66} 17.7

We failed to find data on the photoelasticity tensor needed to calculate the second terms in (8) and (10). Table 1 presents all the numerically calculated coefficients $L_{\mathrm{o,e};\|,\perp}$ and $N_{\mathrm{o,e};\|,\perp}$, for a rod with the aspect ratio 1 : 10 (length 50 mm, diameter 5 mm), which are close to the approximate values

$$L_{\mathrm{o,e};\|,\perp} \approx (n_{\mathrm{o,e}}-1)\alpha\frac{d}{l}, \quad N_{\mathrm{o,e};\|,\perp} \approx \frac{\mathrm{d}n_{\mathrm{o,e}}}{\mathrm{d}T}, \tag{11}$$

where α is the linear thermal expansion coefficient along the sample (along the z axis in Fig. 1); in our geometry, $\alpha = \alpha_{\perp}$.

Table 1 shows that, for a long rod, the third term in (10) in negligibly small compared to the first term for both the

Table 1. Numerically calculated coefficients L, N, and R (in 10^{-6} K^{-1}) for a rod with the aspect ratio 1 : 10.

Polarisation	Astigmatism direction	N	L	$R^{(11)}$	$R^{(12)}$	$R^{(13)}$	$R^{(16)}$	$R^{(31)}$	$R^{(33)}$	$R^{(61)}$	$R^{(66)}$	$R^{(54)}$	$R^{(55)}$
Ordinary	$\|\|c$	−1.91	0.48	−12.3	−1.62	−17.3	−0.95	0	0	0	0	0	0
	$\perp c$	−1.96	0.52	−29.0	−1.83	−2.17	−5.25	0	0	0	0	0	0
Extraordinary	$\|\|c$	−4.1	0.50	0	0	0	0	−14.5	−18.1	0	0	0	0
	$\perp c$	−4.21	0.54	0	0	0	0	−32.3	−2.27	0	0	0	0

ordinary and extraordinary waves. Since the first term determines the negative lens, the appearance of the positive thermal lens observed in [4–7] cannot be explained without the second term (photoelastic effect). The calculation performed disregarding the photoelastic effect for the experimental conditions of [8–12] also yields a negative thermal lens power instead of observed positive. The strong astigmatism of the thermal lens measured in [3–7] also cannot be explained without the photoelastic effect. The anisotropy of the thermal conductivity ($\kappa_{||} = 0.8\kappa_{\perp}$) leads to the relation $|F_{e||}| = 0.8|F_{e\perp}|$, while the focal length $|F_{e||}|$ in all the experiments [3–7] was larger or even much larger than $|F_{e\perp}|$. According to Table 1, the thermal lens astigmatism associated with lengthening of the sample is also negligibly small ($L_{o,e;||} \approx L_{o,e;\perp}$). Thus, the numerous experimental data [3–12] cannot be even qualitatively explained without the photoelastic effect.

4. Influence of the photoelastic effect

The influence of the photoelastic effect can be analysed despite unknown p_{ijkl} for YLF. First of all, we take into account the symmetry group of the YLF crystal (tetragonal, point group 4/m). For this group, the photoelasticity tensor in the Nye two-index notation in the crystallographic coordinate system is given by ten independent photoelastic coefficients [20]:

$$p_{mn} = \begin{pmatrix} p_{11} & p_{12} & p_{13} & 0 & 0 & p_{16} \\ p_{12} & p_{11} & p_{13} & 0 & 0 & -p_{16} \\ p_{31} & p_{31} & p_{33} & 0 & 0 & 0 \\ 0 & 0 & 0 & p_{44} & p_{45} & 0 \\ 0 & 0 & 0 & -p_{45} & p_{44} & 0 \\ p_{61} & -p_{61} & 0 & 0 & 0 & p_{66} \end{pmatrix}, \quad m, n = 1, ..., 6. \tag{12}$$

To obtain the tensor in the laboratory coordinate system, we should use the tensor rotation formula. Since the second term in (8) is linear in the tensor p_{ijkl}, it is obvious that the second term in (10) can be represented in the form

$$E_{o,e;||,\perp} = \sum_{n,m=1}^{6} R^{(mn)}_{o,e;||,\perp} p_{mn}, \tag{13}$$

where coefficients R are determined by the elasticity and linear expansion tensors. This allows us to consider the effect of all the ten photoelastic coefficients on the thermal lens independently of each other. Successively equating to zero nine of the ten photoelastic coefficients, we numerically find all the coefficients R (see Table 1). Since (8) contains only the diagonal elements of the tensor B, the form of the elasticity tensor (12) reveals that the coefficients p_{44}, p_{45}, p_{61} and p_{66} do not affect the thermal lens. The numerical calculation shows that the contribution of p_{12} can also be neglected.

Thus, considerable contributions to the thermal lens in a long a-cut YLF rod are made only by five of the ten photoelastic coefficients p_{mn}, three of them (p_{11}, p_{13}, p_{16}) affecting only the ordinary wave and two coefficients (p_{31}, p_{33}) affecting only the extraordinary wave. Therefore, it is enough to know only p_{11}, p_{13} and p_{16}, for lasers emitting the

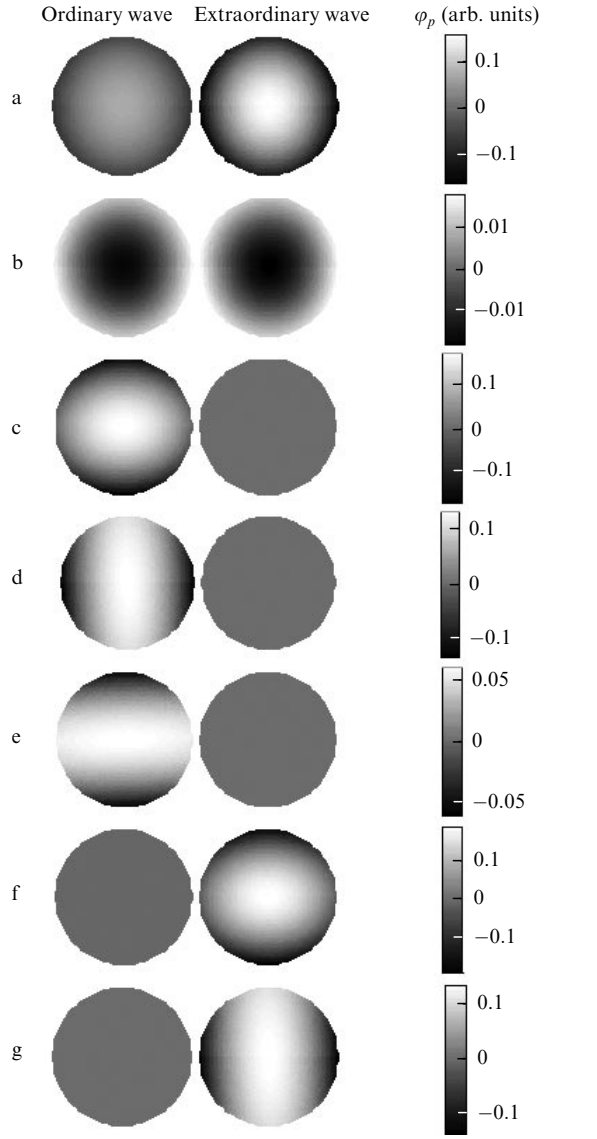

Figure 2. Calculated transverse distributions of the thermally induced phase of radiation passed through a long YLF rod with the aspect ratio 1 : 10 for a volume-uniform heat source with the power $P_{heat} = 1$ W. The optical axis c lies in the plane of the rod face. The thermal lens is caused by the temperature dependence of the refractive index (a), by thermal expansion (b), and by the photoelastic effect with nonzero photoelastic coefficients $p_{11} = 0.1$ (c), $p_{13} = 0.1$ (d), $p_{16} = 0.1$ (e), $p_{31} = 0.1$ (f), and $p_{33} = 0.1$ (g).

Table 2. Photoelastic coefficients p_{mn}, which allow interpretation of the experimental data [3–7], and coefficients $E_{o,e;||,\perp}$ calculated by formula (13).

p_{11}	p_{13}	p_{16}	p_{31}	p_{33}	$E_{o\|\|}$ (10^{-6} K^{-1})	$E_{o\perp}$ (10^{-6} K^{-1})	$E_{e\|\|}$ (10^{-6} K^{-1})	$E_{e\perp}$ (10^{-6} K^{-1})
−0.04	−0.04	−0.05	−0.06	−0.15	1.2	1.5	3.6	2.3

ordinary wave ($\lambda = 1053$ nm for the Nd : YLF crystal) and p_{31}, p_{33} for lasers emitting the extraordinary wave ($\lambda = 1047$ nm for Nd : YLF). Figure 2 shows the thermally-induced phase distribution in an YLF rod 50 mm long and 5 mm in diameter, which are determined by different components of the photoelasticity tensor, as well as by the temperature dependence of the refractive index and by the thermal expansion.

Using the photoelastic coefficients as fitting parameters, we correlated the numerical calculations results with the experimental data of [3–7]. This is a rather difficult problem because the heat release power P_{heat} is not known exactly and can only be estimated from the pump power with an accuracy to coefficients ~ 2 for diode pumping and ~ 5 for lamp pumping. Within this uncertainty, the heat release power was also used as a fitting parameter. With this statement of the problem, we managed to qualitatively interpret 24 experiments [3–7] (six geometries and four focal lengths $F_{o,e;||,\perp}$ in each of them) using 11 fitting parameters (six values of the heat release power and five photoelastic coefficients). The results are listed in Table 2. This proves that all the specific features (including the strong astigmatism) of the thermal lens in the YLF crystal can be explained with the help of the photoelastic effect.

The values of p_{mn} presented in Table 2 do not claim to be highly accurate since they are obtained by fitting to different experimental data whose accuracy is unknown. In addition, we did not take into account that some experiments were performed at the wavelength $\lambda = 1053$ nm and the others at $\lambda = 633$ nm. To determine p_{mn} precisely, we need additional experiment. At the same time, the parameters of the thermal lens in a long YLF rod can be estimated quite accurately by formulae (9), (10) using expressions (11) and values of $E_{o,e;||,\perp}$ given in Table 2.

5. Conclusions

In this work, we have proved that the astigmatism of the thermal lens in the YLF crystal is caused solely by the photoelastic effect. The photoelastic effect does not change the intrinsic polarisations of crystals with natural anisotropy but substantially changes the refractive indices for radiation with these polarisations. These changes are principally astigmatic since the angle between the optical axis and the temperature gradient is different at different points of the crystal cross section.

We have precisely calculated the thermal lens in an *a*-cut YLF rod taking into account the anisotropy of the thermal conductivity, elasticity, linear expansion, and refractive index. It is proved that the numerous experimental data cannot be even qualitatively explained neglecting the photoelastic effect. It is shown that the contribution to the thermal lens is made only by three photoelastic coefficients (p_{11}, p_{13}, p_{16}) for the ordinary wave and only by two coefficients (p_{31}, p_{33}) for the extraordinary wave. Using these five coefficients as fitting parameters, we quantitatively interpreted all available experimental data. Simple formulae for estimation of the thermal lens parameters in an YLF rod have been presented.

In the future, we plan to generalise the obtained results to the disc geometry, to an arbitrary orientation of the YLF crystal axes, and to other crystals, including crystals of other symmetry groups.

References

1. Mezenov A.V., Soms L.N., Stepanov A.I. *Termooptika tverdotel'nykh lazerov* (Thermooptics of Solid-State Lasers) (Leningrad: Mashinostroenie, 1986).
2. Koechner W. *Solid-State Laser Engineering* (Berlin: Springer, 1999).
3. D'yakova A.F., Kornev A.F., Reiterov V.M., Soms L.N., Stupnikov V.K., Tkachuk A.M., Ushakova O.A. *Izv. Akad. Nauk SSSR. Ser. Fiz.*, **55**, 294 (1991).
4. Skeldon M.D., Saager R.B., Seka W. *IEEE J. Quantum Electron.*, **35**, 381 (1999).
5. Cerullo G., De Silvestri S., Magni V. *Opt. Commun.*, **93**, 77 (1992).
6. Vanherzeele H. *Opt. Lett.*, **13**, 369 (1988).
7. Hardman P.J., Clarkson W.A., Friel G.J., Pollnau M., Hanna D.C. *IEEE J. Quantum Electron.*, **35**, 647 (1999).
8. Murray J.E. *IEEE J. Quantum Electron.*, **19**, 488 (1983).
9. Clarkson W.A., Hardman P.J., Hanna D.C. *Opt. Lett.*, **23**, 1363 (1998).
10. Pfistner C., Weber R., Weber H.P., Merazzi S., Gruber R. *IEEE J. Quantum Electron.*, **30**, 1605 (1994).
11. Peng X., Asundi A. *IEEE J. Quantum Electron.*, **41**, 5361 (2005).
12. Peng X., Asundi A. *Appl. Opt.*, **44**, 800 (2005).
13. Landau L.D., Lifshits E.M. *Mekhanika* (Mechanics) (Moscow: Nauka, 2004).
14. Koechner W., Rice D.K. *J. Opt. Soc. Am.*, **61**, 758 (1971).
15. Hirano Y., Yanagisawa T., Tajime T., Uchino O., Nagai T., Nagasawa C. *Opt. Lett.*, **25**, 1168 (2000).
16. Katin E.V., Lozhkarev V.V., Palashov O.V., Khazanov E.A. *Kvantovaya Elektron.*, **33** (9), 836 (2003) [*Quantum Electron.*, **33** (9), 836 (2003)].
17. Potemkin A.K., Katin E.V., Kirsanov A.V., Luchinin G.A., Malshakov A.N., Mart'yanov M.A., Matveev A.Z., Palashov O.V., Khazanov E.A. Shaikin A.A. *Kvantovaya Elektron.*, **35** (4), 302 (2005) [*Quantum Electron.*, **35** (4), 302 (2005)].
18. Blistanov A.A. *Kristally kvantovoi i nelineinoi optiki* (Crystals of Quantum and Nonlinear optics) (Moscow: MISIS, 2000).
19. Martienssen W., Warlimont H. (Eds) *Handbook Springer of Condensed Matter and Materials Data* (Berlin – Heidelberg: Springer, 2005).
20. Nye J.F. *Physical Properties of Crystals: Their Representation by Tensors and Matrices* (Clarendon Press, Oxford, 1957; Moscow: Inostr. Literatura, 1960).